

Polysaccharide source altered ecological network, functional profile, and short-chain fatty acid production in a porcine gut microbiota

C. Long, S. de Vries and K. Venema

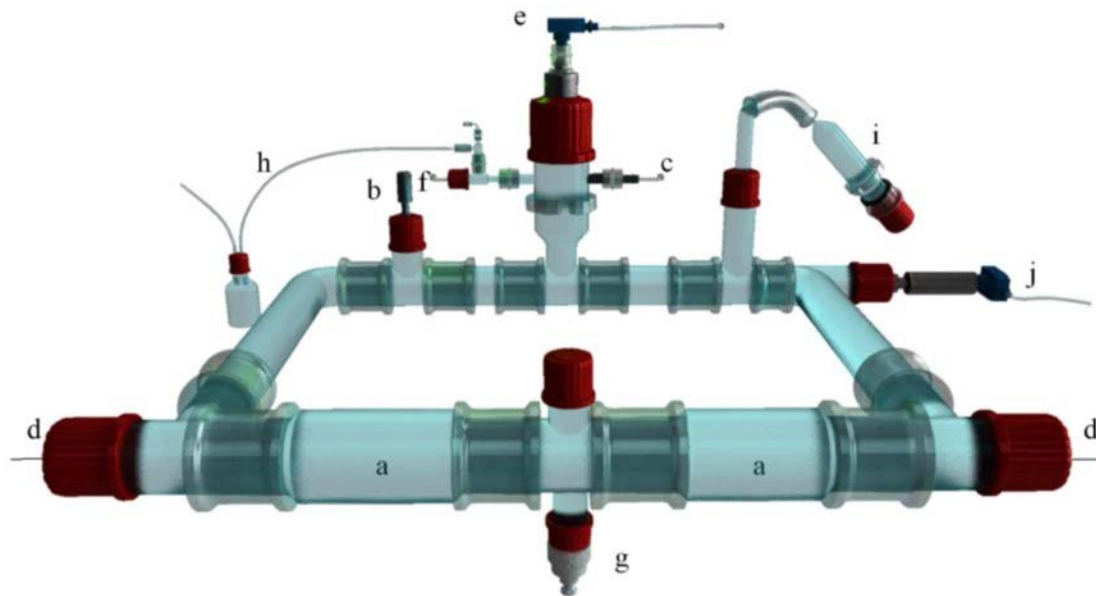


Figure S1. SLIM schematic, modified from Minekus *et al.* (1999).

(a) peristaltic compartments with a hollow fiber membrane inside, (b) pH sensor, (c) NaOH secretion, (d) dialysate system, (e) level sensor, (f) gaseous N₂ inlet, (g) sampling port, (h) gas outlet, (i) test compound + SIEM feeding syringe, (j) temperature sensor.

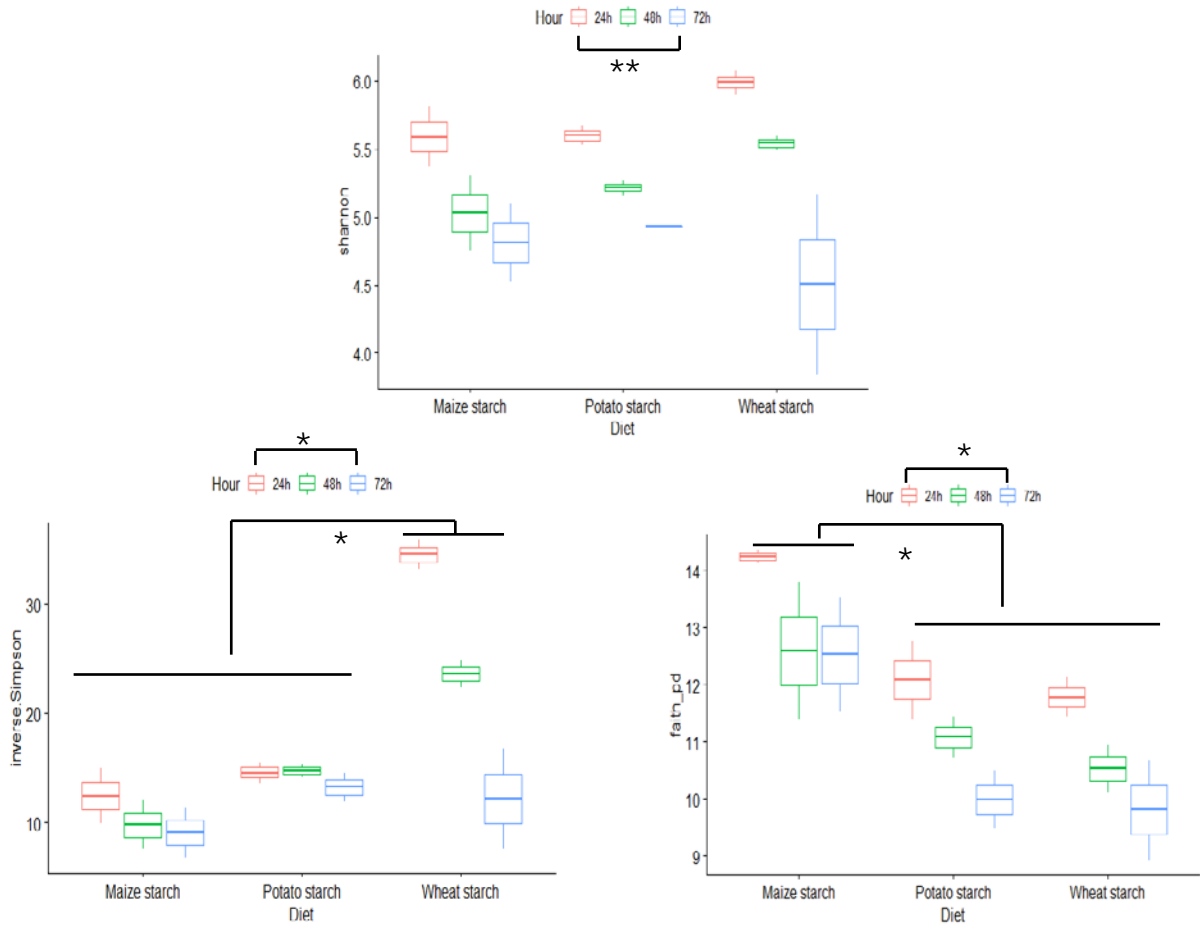


Figure S2. The effect of starch source and fermentation time on alpha diversity indices (Shannon, inverse Simpson and Faith_PD).

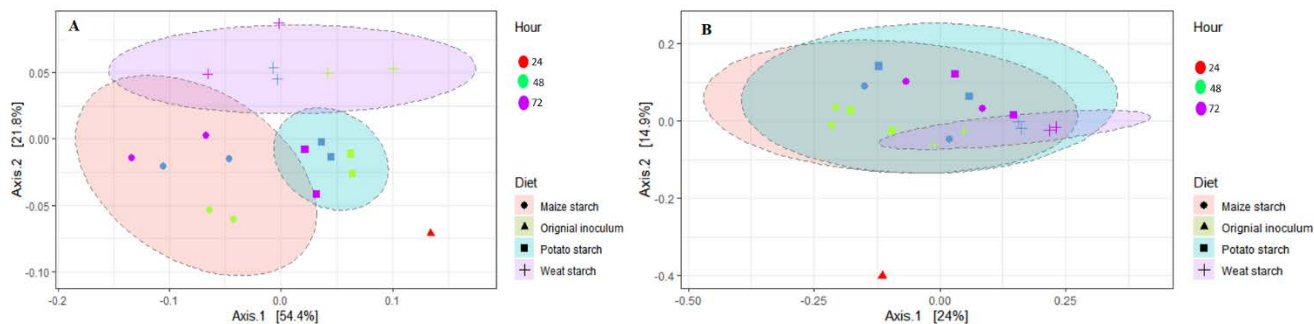


Figure S3. Principal coordinate analysis plots generated based on the calculated distances in a weighted (A) and unweighted (B) UniFrac matrix.

Samples were grouped by colour (time-points) and shape (in terms of diet group) they belonged to. The ellipses were drawn at the 0.95 confidence level. Diet sources and original were significant different from each other, for weighted uniFrac: original inoculum to maize starch ($P=0.041$), to potato starch ($P=0.031$), to wheat starch ($P=0.033$); maize starch to potato starch ($P=0.002$), to wheat starch ($P=0.002$); for unweighted uniFrac: original inoculum to maize starch ($P=0.046$), to potato starch ($P=0.041$), to wheat starch ($P=0.048$); maize starch to potato starch ($P=0.022$), to wheat starch ($P=0.006$).

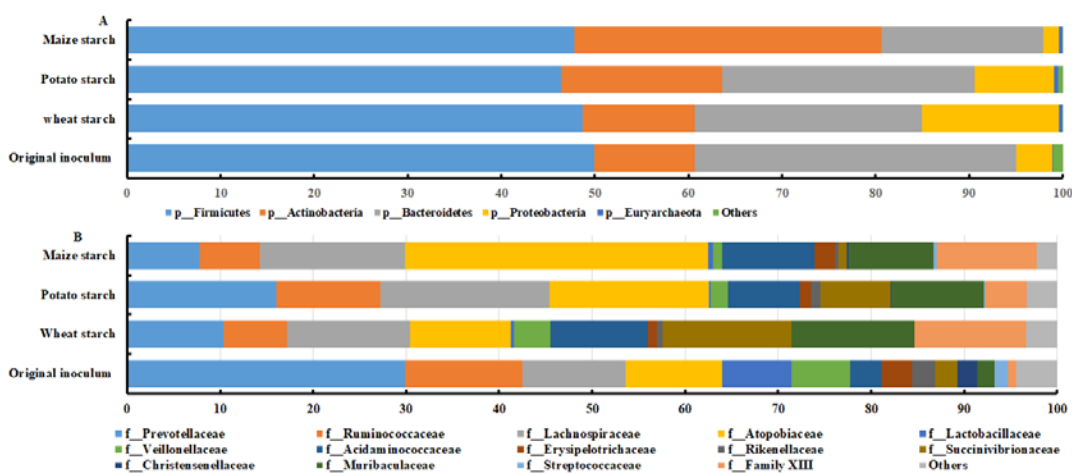


Figure S4. Relative abundances of microbial phyla (A) and families (B) in the original inoculum, and microbiota fed with different starches.

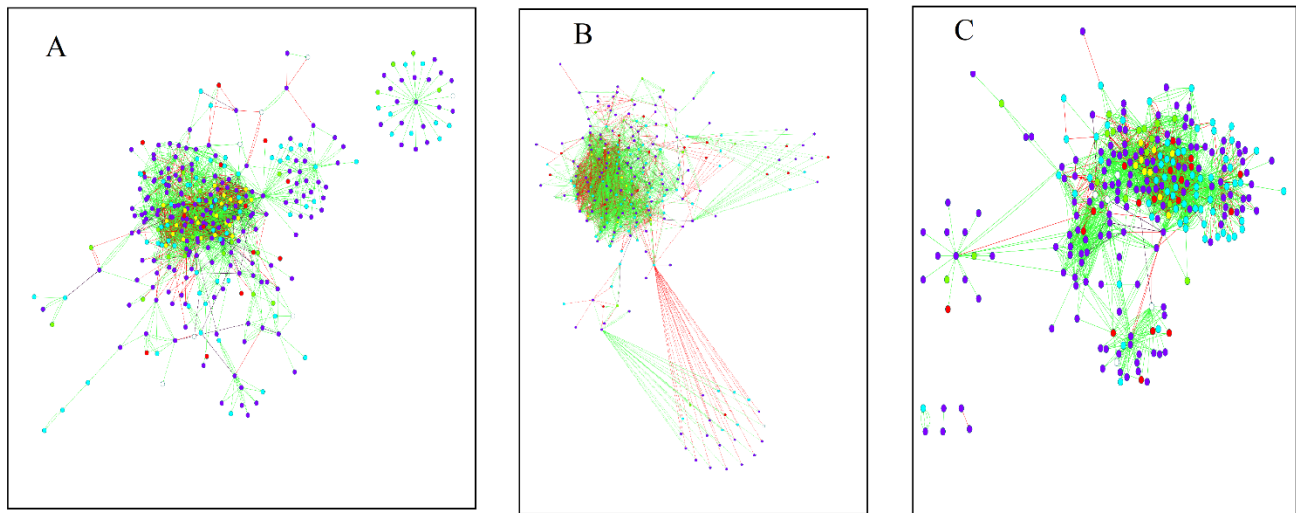


Figure S6. Co-occurrence networks in the porcine gut microbiome. (A) Maize-starch-based network. (B) Potato-starch-based network. (C) Wheat-starch-based network.

Modules were detected by using MCODE in Cytoscape. Each color represents a module. Green edges represent positive interaction, while red ones represent negative interaction, and black ones are unknown.

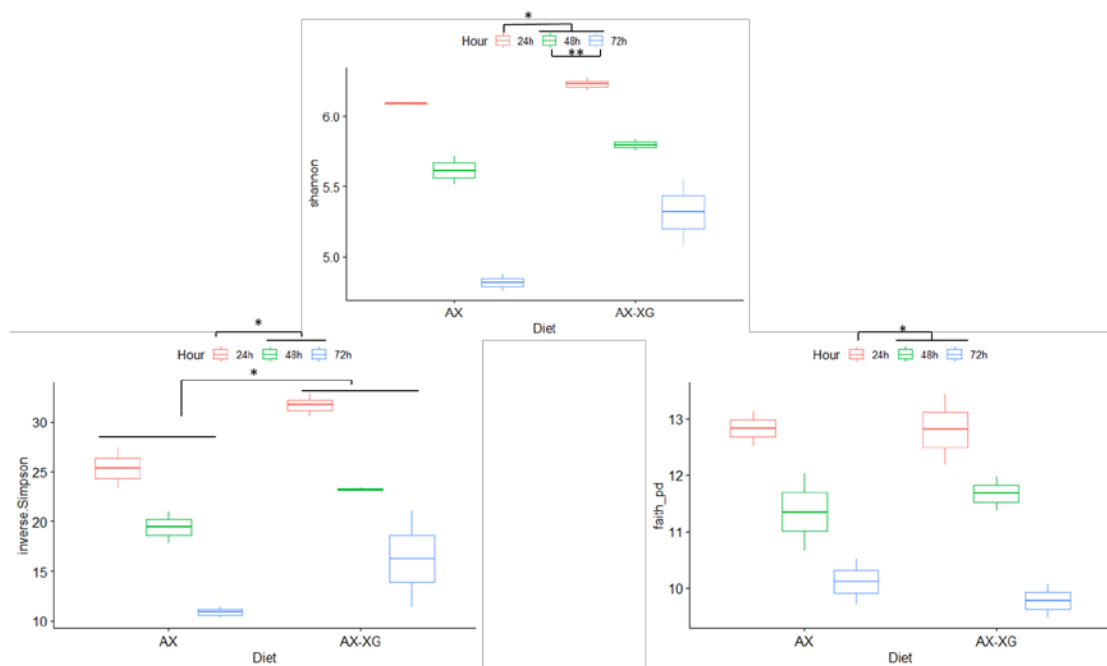


Figure S7. The effect of non-starch polysaccharides and fermentation time on alpha diversity indices (Shannon, inverse Simpson and Faith_PD).

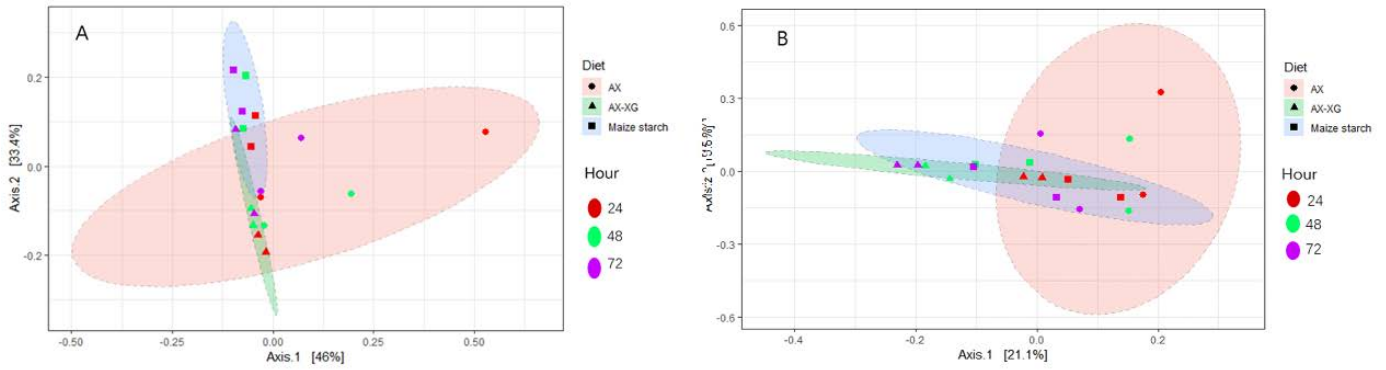


Figure S8. Principal coordinate analysis (PCoA) plots generated based on the calculated distances in a weighted (A) and unweighted (B) UniFrac matrix.

Samples were grouped by colour (time-point) and shape (in terms of diet group) they belonged to. The ellipses were drawn at the 0.95 confidence level. Weighted: AX to AX-XG ($P=0.003$), AX-XG to maize starch ($P=0.003$), AX to maize starch ($P=0.003$); Unweighted: AX to AX-XG ($P=0.034$), AX-XG to maize starch ($P=0.024$), AX to maize starch ($P=0.141$).

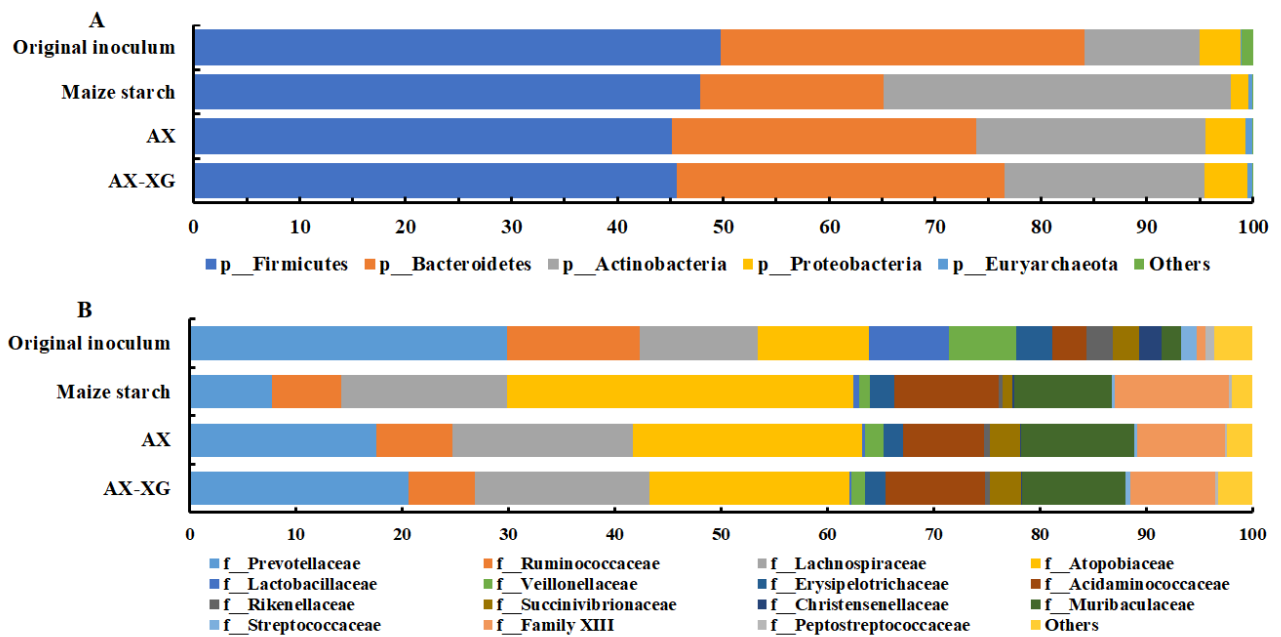
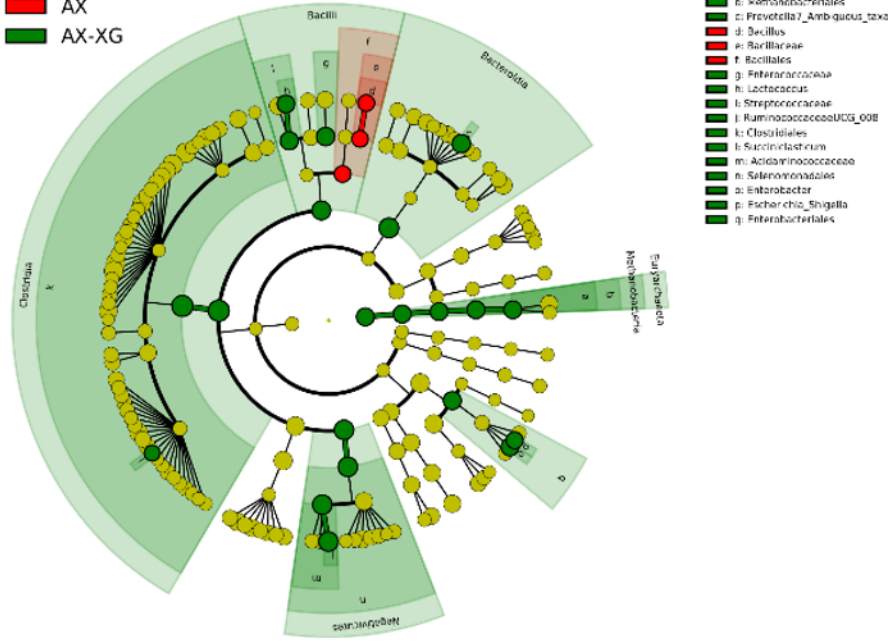


Figure S9. Relative abundances of microbial phyla and families in the original inoculum and microbiota fed with maize starch, AX, and AX-XG.

A

■ AX
■ AX-XG



B

■ AX ■ AX-XG

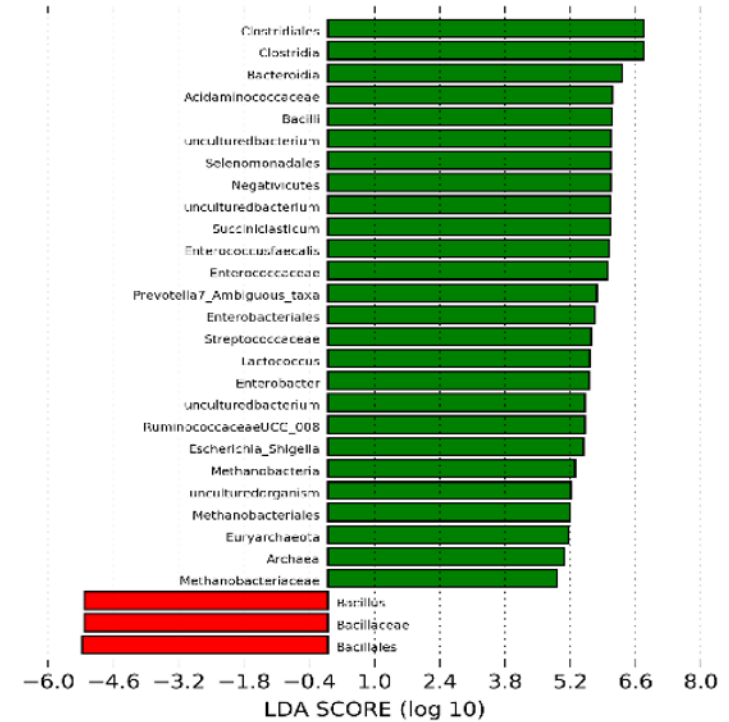


Figure S10. LEfSe results on the microbiome of AX and AX-XG group. (A) Taxonomic representation of statistically and biologically consistent differences between AX and AX-XG groups. (B) Histogram of the LDA scores computed for features differentially abundant between AX and AX-XG group.

Differences in the most abundance taxa are indicated, red indicating significantly higher in the AX group, green indicating significantly higher in the AX-XG group.